

Energy flows from one form to another...

GRAVITATIONAL POTENTIAL ENERGY



KINETIC ENERGY



HEAT



RADIATION

If the disc radiates like a Blackbody

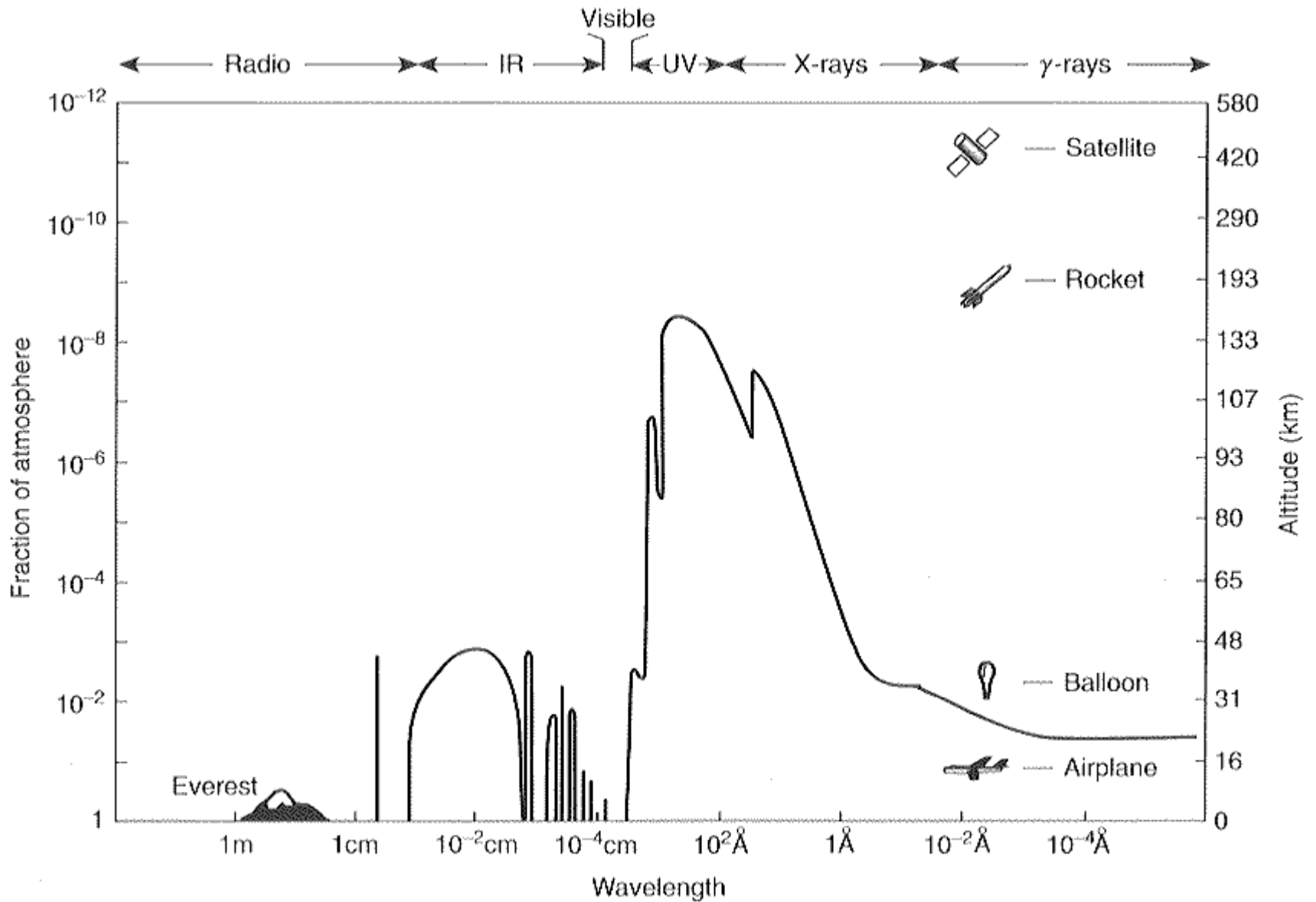
$$L_E = T^4 4\pi r^2 \sigma_{\text{Stefan-Boltzmann}}$$

We assume as „ r “ the last stable orbit around the black hole

$$T = 2 \times 10^7 M^{-1/4} \text{ K}$$

	M (solar masses)	T (K)	λ (Angstrom)	
Microquasar	3	$1.5 \cdot 10^7$	2	X-ray
AGN	10^9	10^5	300	uv

The reason for the delay in discovering the much closer to us microquasars is the fact that their disc emits in X-rays and our atmosphere is opaque at these wavelengths.



Absorption of electromagnetic radiation by the atmosphere

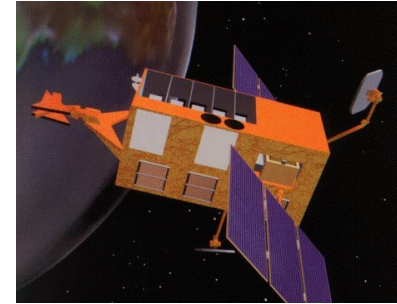
1962: Giacconi et al. discovery of Sco X-1

1967: Discovery of radio pulsars.

1970: First astronomy satellite, an X-ray mission called Uhuru, was launched.

- Uhuru, Einstein, ROSAT, ASCA, BeppoSAX, RXTE, XMM, Chandra

- -Rossi X-ray Timing Explorer (RXTE) - NASA, launched 1995
- - very large collecting area in energy range 2-100 keV
- - very high time resolution
- - reasonable spectroscopy
- - enormous field of view, but no images



- -X-ray Multi-Mirror Mission (XMM-Newton) - ESA, launched 1999
- - large collecting area in range 0.2-12 keV
- - reasonable time resolution
- - high-resolution spectroscopy up to few keV
- - 10 arcsec resolution over 30' FOV



- - Chandra X-ray Observatory (AXAF, CXO) - NASA, launched 1999
- - modest collecting area in range 0.5-10 keV
- - high time resolution
- - very high-resolution spectroscopy up to few keV
- - 0.9 arcsec resolution over 16' FOV



Swift is a multi-wavelength space-based observatory: gamma-ray, X-Ray, UltraViolet Optical telescope

HEAO A-1 ALL-SKY X-RAY CATALOG

NAVAL RESEARCH LABORATORY

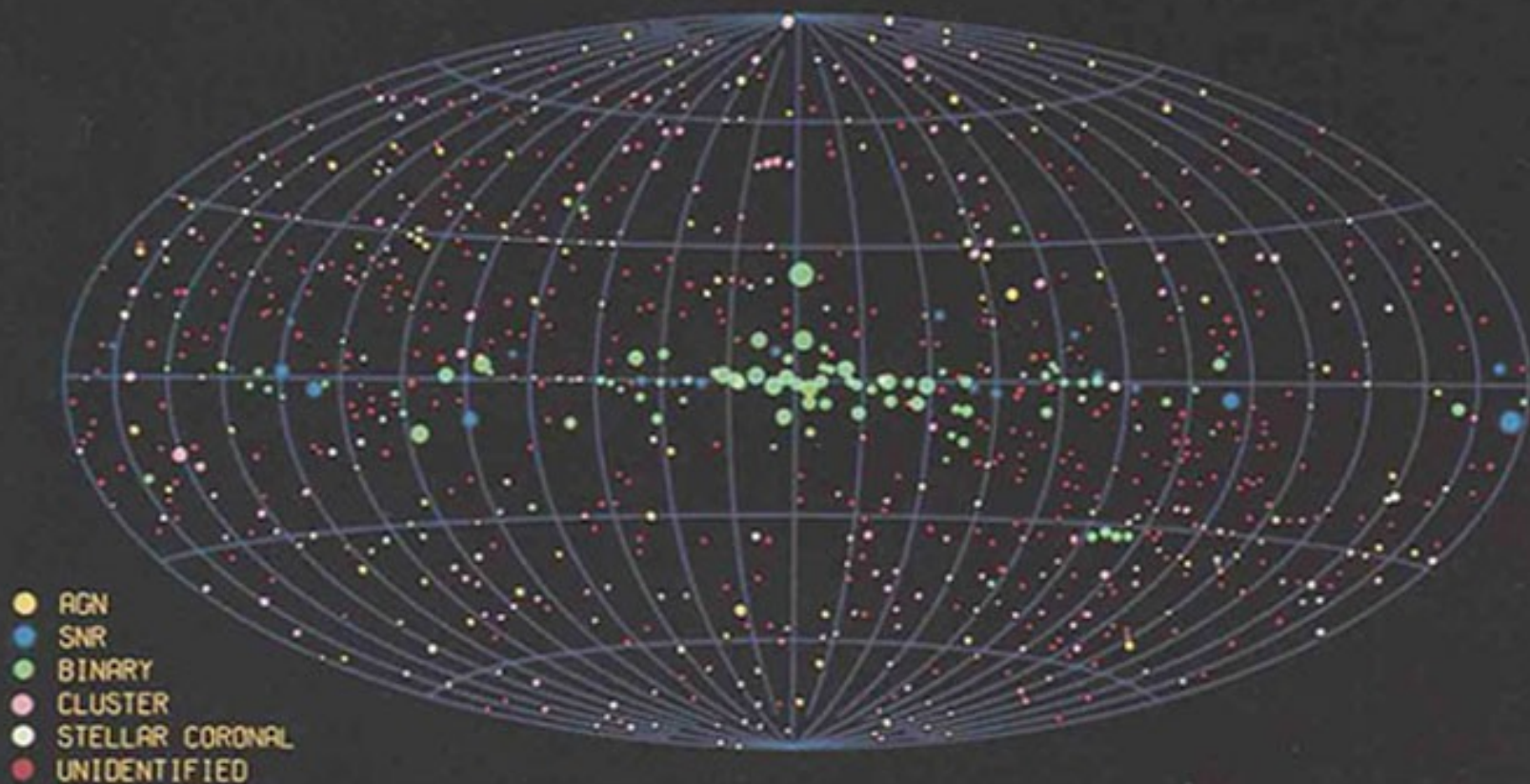


Fig. 1.7 Map showing X-ray sources from the HEAO-1 all-sky survey. Size of the dot shows the brightness of the source. Colours indicate type of source. (Courtesy of K. Wood, NRL.)

Where are the other objects like SS433 ?

Margon 1980,1984

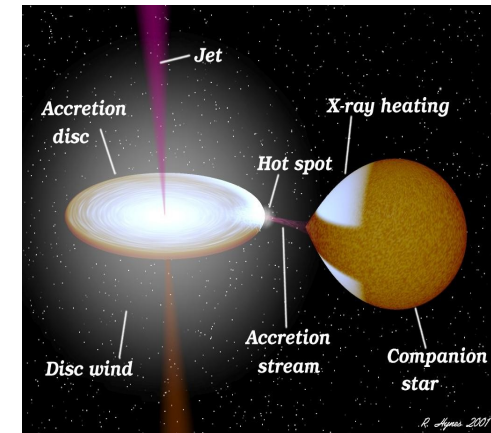
Radio-loud X-ray Binaries:

MICROQUASARS:

SS433	Margon 1979, Spencer 1979
1E1740-2942	Mirabel et al. 1992
GRS1758-258	Rodriguez et al. 1992
Cygnus X-3	elongation Geldzahler et al. 1983
	Spencer et al 1986
	Schalinski et al. 1990, 1995
Circinus X-1	Stewart et al. 1993
LS I 61303	Massi et al. 1993
GRS1915+105	Mirabel & Rodriguez 1994
GROJ1655-40	Tingay et al. 1995; Hjellming & Rupen 1995
XTEJ1748-288	Hjllming et al. 1998
CI Cam	Mioduszewski et al. 1998
LS 5039	Paredes et al. 2000
V461 Sgr	Hjllming et al. 2000
Cygnus X-1	Stirling et al. 2001
Sco X-1	Fomalont et al. 2001
XTEJ1550-564	Hannikainen et al. 2001
XTEJ1859+226	Brocksopp et al. 2002

INVERTED/ FLAT SPECTRUM COMPACT SOURCES:

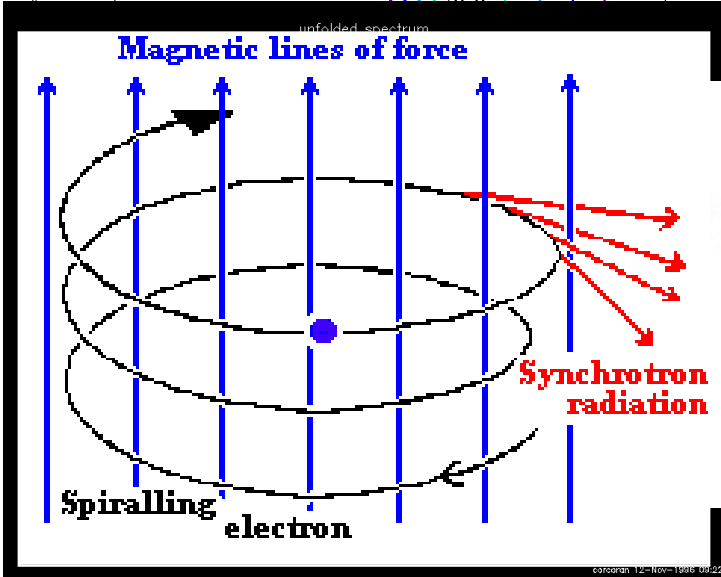
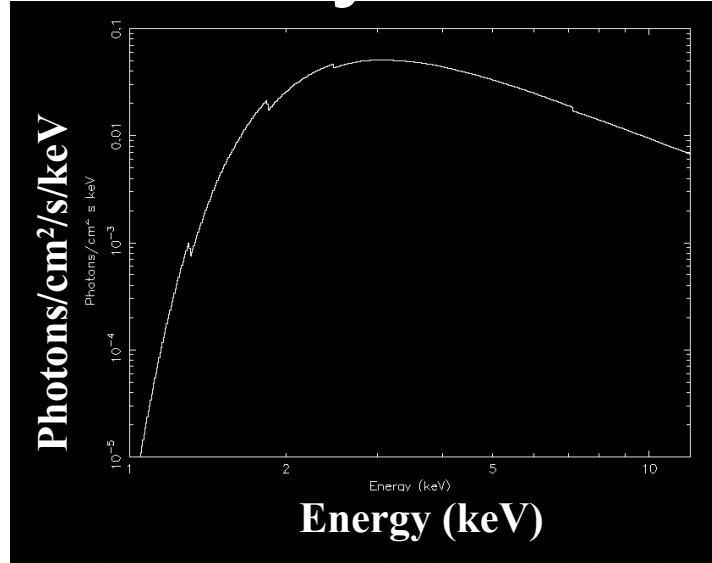
GX339-4	Fender et al. 1997, recently resolved by Gallo et al. 2004
XTEJ1118+480	Fender et al. 2001



- Energy range $\approx 0.1 - 500$ keV (“soft”, “hard”)
- Flux: $F = 3 \times 10^{-12}$ ergs/cm²/s over 0.2-10 keV
- Luminosity: $L = 4\pi D^2 F = 4 \times 10^{37}$ ergs/s
- Flux density: 2×10^{-4} ph/cm²/s/keV at 1 keV

- Thermal emission:
 - blackbody
 - bremsstrahlung
 - emission/absorption lines (inner electrons)

- Non-thermal emission
 - synchrotron
 - inverse Compton



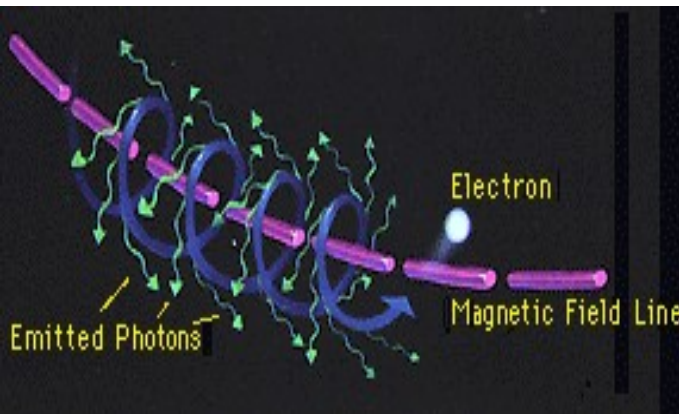
e

Magnetic field

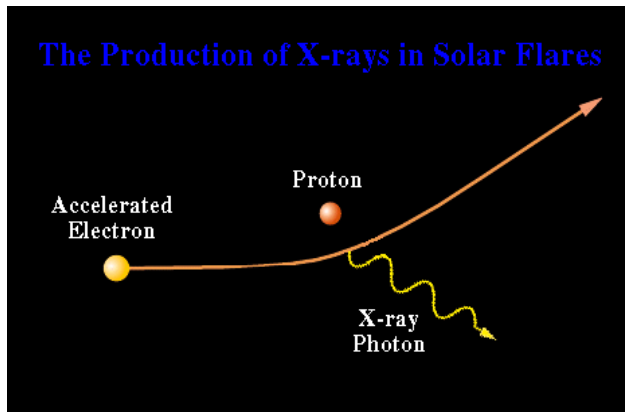
Matter

Radiation field

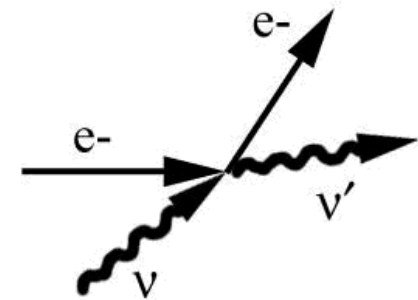
by synchrotron radiation



- Bremsstrahlung
- emission



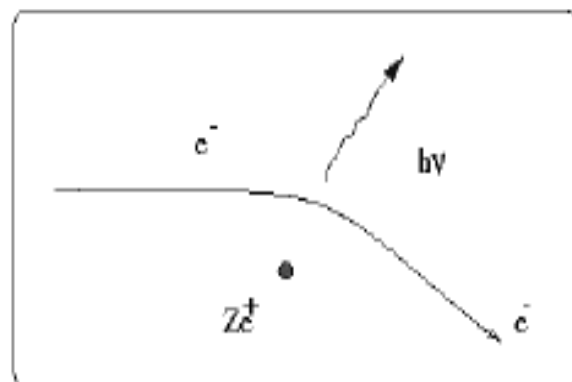
Inverse Compton scattering



$\nu' > \nu$
High energy e^- initially
 e^- loses energy

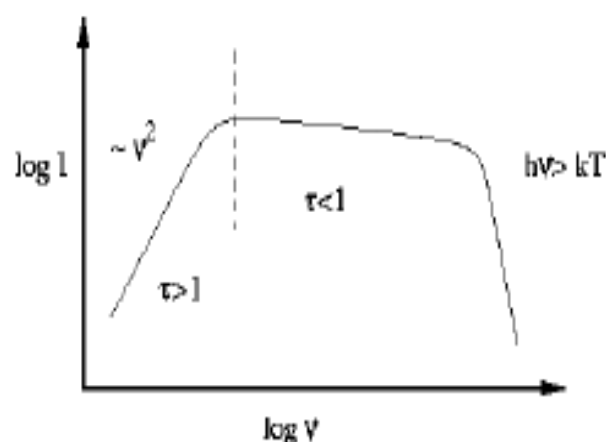
Thermal bremsstrahlung (free-free) radiation

- Thermal radiation produced by charged particles as they are accelerated through Coulomb interactions with other charges.



Thermal bremsstrahlung (iii)

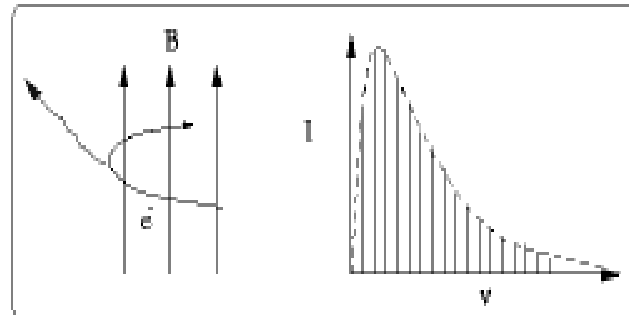
- Importantly then, at low frequencies (e.g. cm radio wavelengths) thermal bremsstrahlung is often seen to be self-absorbed.



- This type of radiation is typically seen in hot ionised plasmas, eg HII regions ($T \sim 10^4\text{K}$), binary x-ray sources ($T \sim 10^7\text{K}$), and the hot inter-galactic medium in clusters of galaxies ($T \sim 10^8\text{K}$).

Synchrotron radiation

- Non-thermal emission from relativistic particles in a magnetic field.

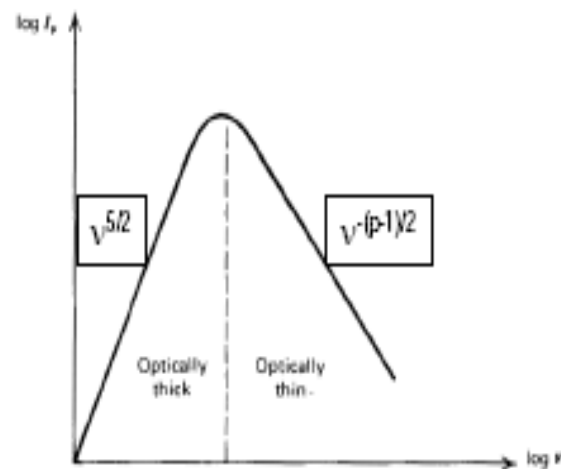


- For a single electron, radiation occurs at finely spaced multiples of the gyro-frequency, $\omega_g = 2\pi\nu_g = eB/\gamma m_g$.
- This emission is polarised, with a peak in the intensity spectrum at $\nu_{\text{max}} \sim \gamma^3 \nu_g$, and a total radiated power that scales like $\sin^2(\theta) \gamma^3 B^2$, with θ the pitch angle between v_{electron} and B .

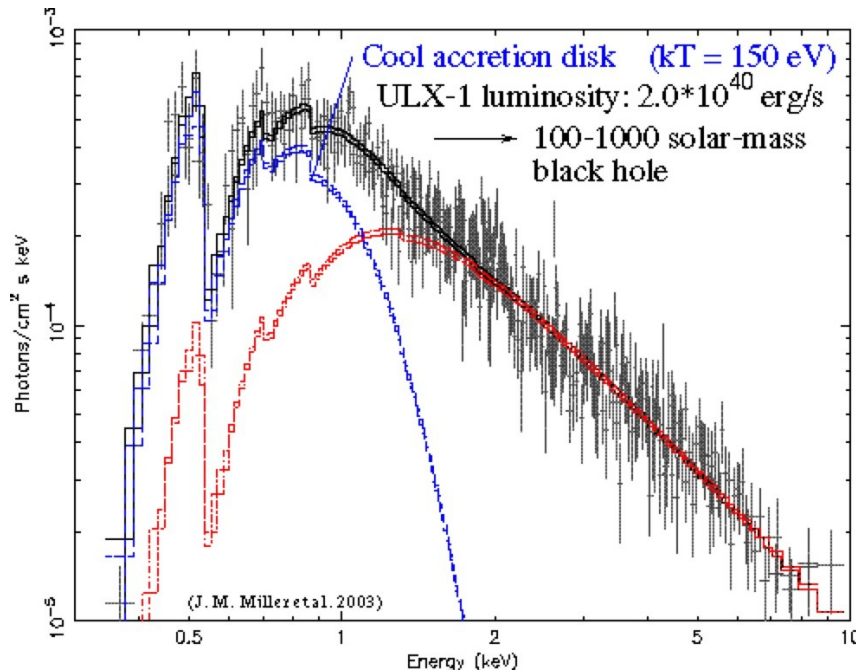
Synchrotron spectra

- Importantly, then, the medium becomes optically thick. It can be shown that, regardless of the energy spectrum of the electrons, the specific intensity in the optically thick region $\propto \nu^{5/2}$. We thus observe a steep, rising spectrum at low ν .
- Since the emission is from a non-thermal population, this optically thick component of the spectrum differs from the ν^2 behaviour of the Rayleigh-Jeans law.

The production of synchrotron radiation is indicative of the presence of violent particle acceleration + B fields. It is seen within the Galaxy, and also in supernova remnants, pulsars, external AGN, radio sources, gamma-ray bursters etc.



X-ray observations



Complex X-ray spectra:

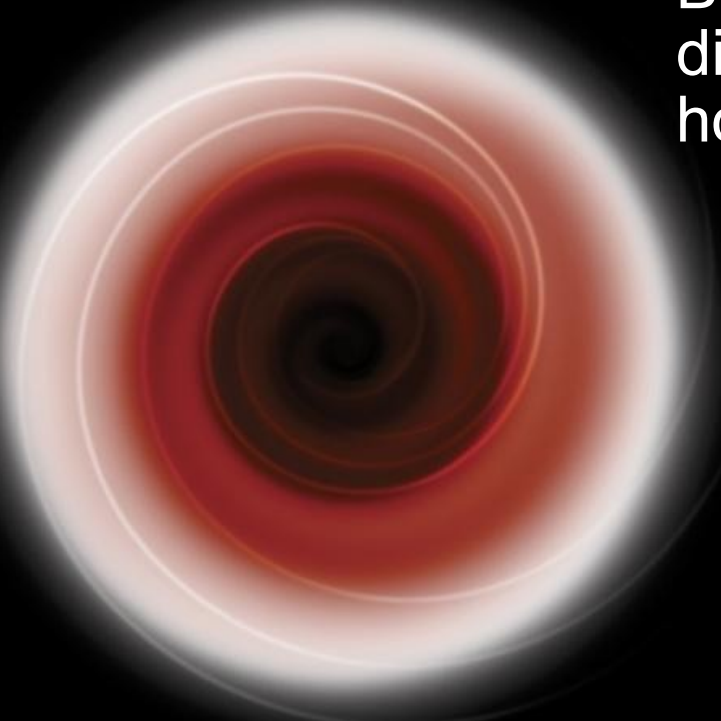
Power-law component with $\Gamma=1-2$ (hot corona + Compton scattering)

Black-body component at soft energies (<1 keV; accretion disk)

- Also variability, high/low states, absorption etc...

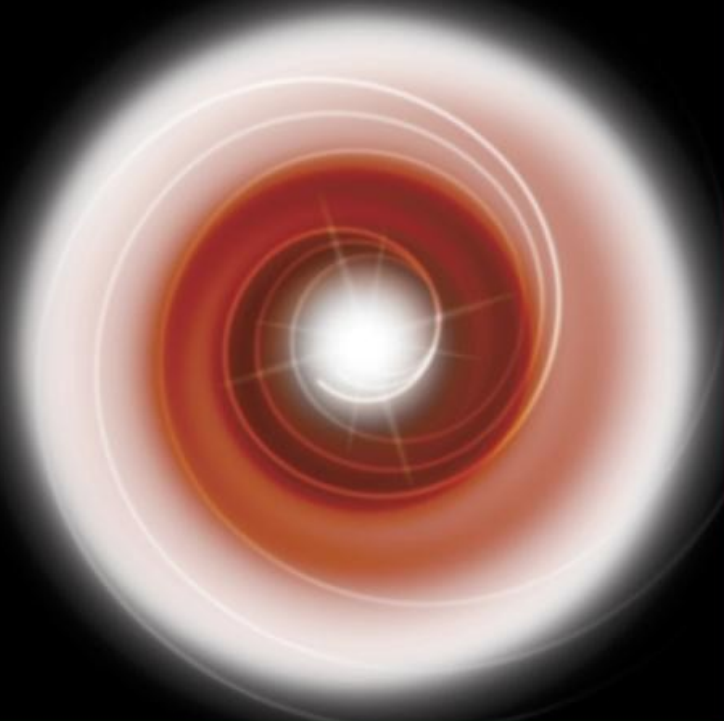
Black-Hole vs. Neutron-Star Binaries

Black Hole X-ray Nova



Black Holes: Accreted matter disappears beyond the event horizon without a trace.

Neutron Star X-ray Nova



Neutron Stars: Accreted matter produces an X-ray flash as it impacts on the neutron star surface.

Classification of Bursts

Type I

- nuclear flashes in surface layers
 - ➔ *nuclear energy*
- Energy proportional to preceding inactivity period
- Burning accumulated material
- spectral softening during decay

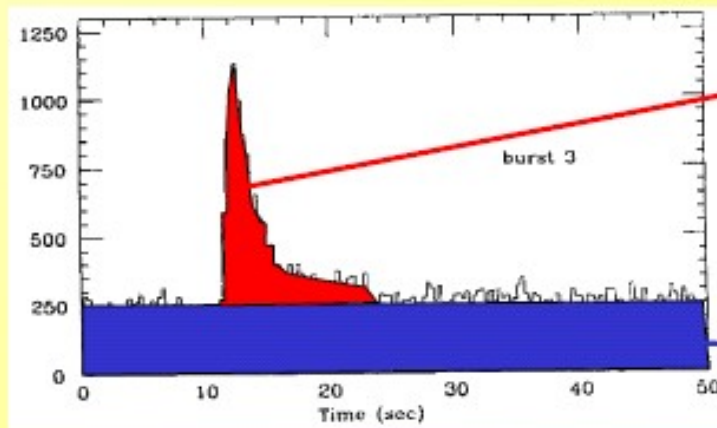
Surface

Type II

- caused by accretion instabilities
 - ➔ *gravitation energy*
- Energy proportional to following inactivity period
- Need to re-fill before regular accretion
luminosity resumes

DISK

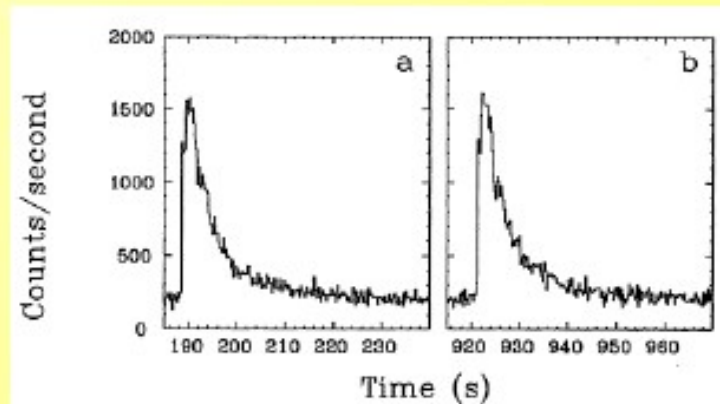
- X-ray bursts occur on the surface of a NS in a LMXB
- type I bursts are caused by thermonuclear reactions



**Burst energy
(thermonuclear energy)**

**Persistent flux
(gravitational energy)**

- main characteristics:
 - fast rise
 - exponential decay
 - spectral softening

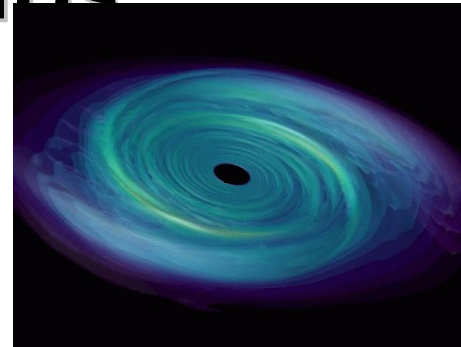


Ron Remillard

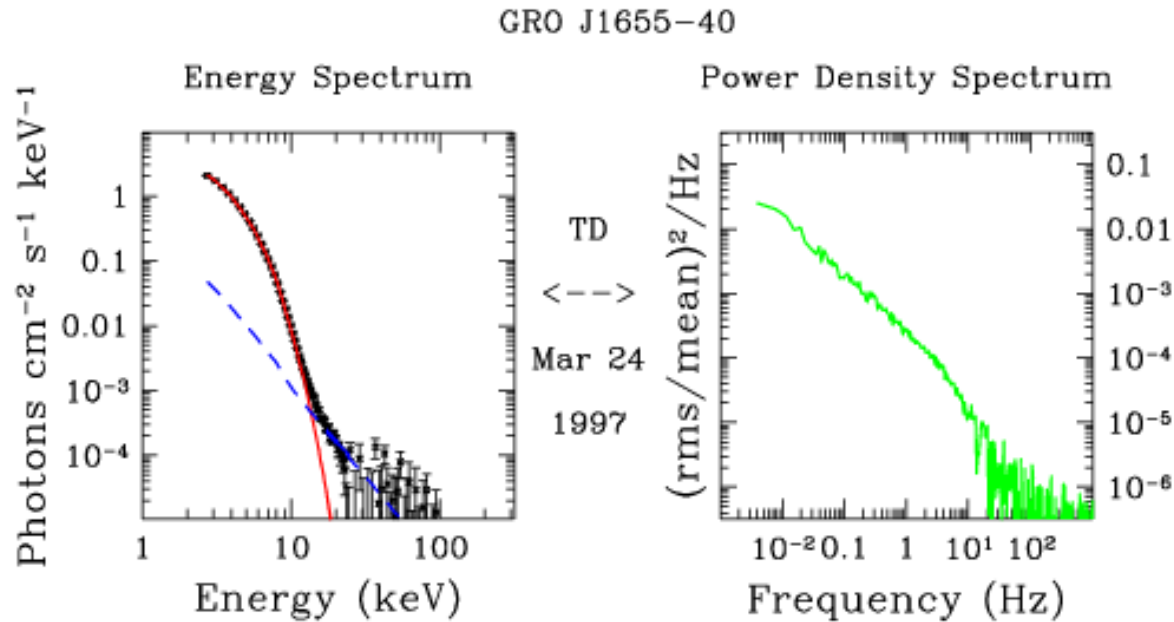
Kavli Center for Astrophysics and Space Research
Massachusetts Institute of Technology

http://xte.mit.edu/~rr/rr_8.971.ppt

X-ray States of BHs



- **Thermal State:**
inner accretion disk

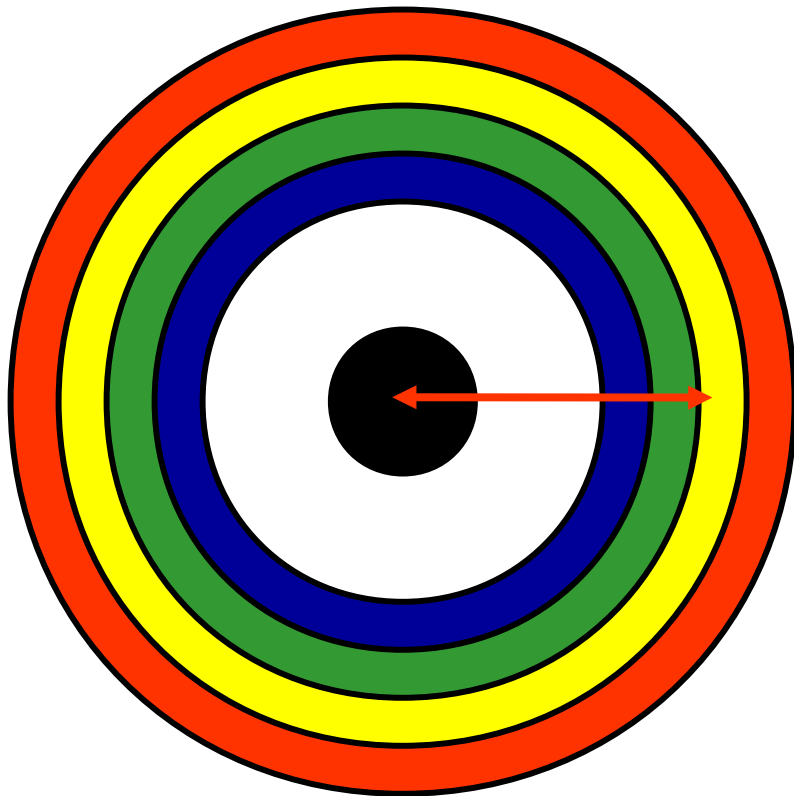


Energy spectra

Power density spectra

Accretion Disk Structure

The accretion disk (AD) can be considered as rings or annuli of blackbody emission.



blackbody flux

$$= \sigma T^4 (R)$$

Model:

multi-temperature (multicolor)
disk

used to describe thermal
component in x-ray spectra

total disk luminosity in steady
state

Very High State (VHS)

strong ultra-soft (US) component and unbroken power-law (PL) component; strong QPOs at $\sim 10\text{Hz}$

High/Soft State (HS)

US dominates; very weak PL component; high luminosity; MCD

Intermediate State

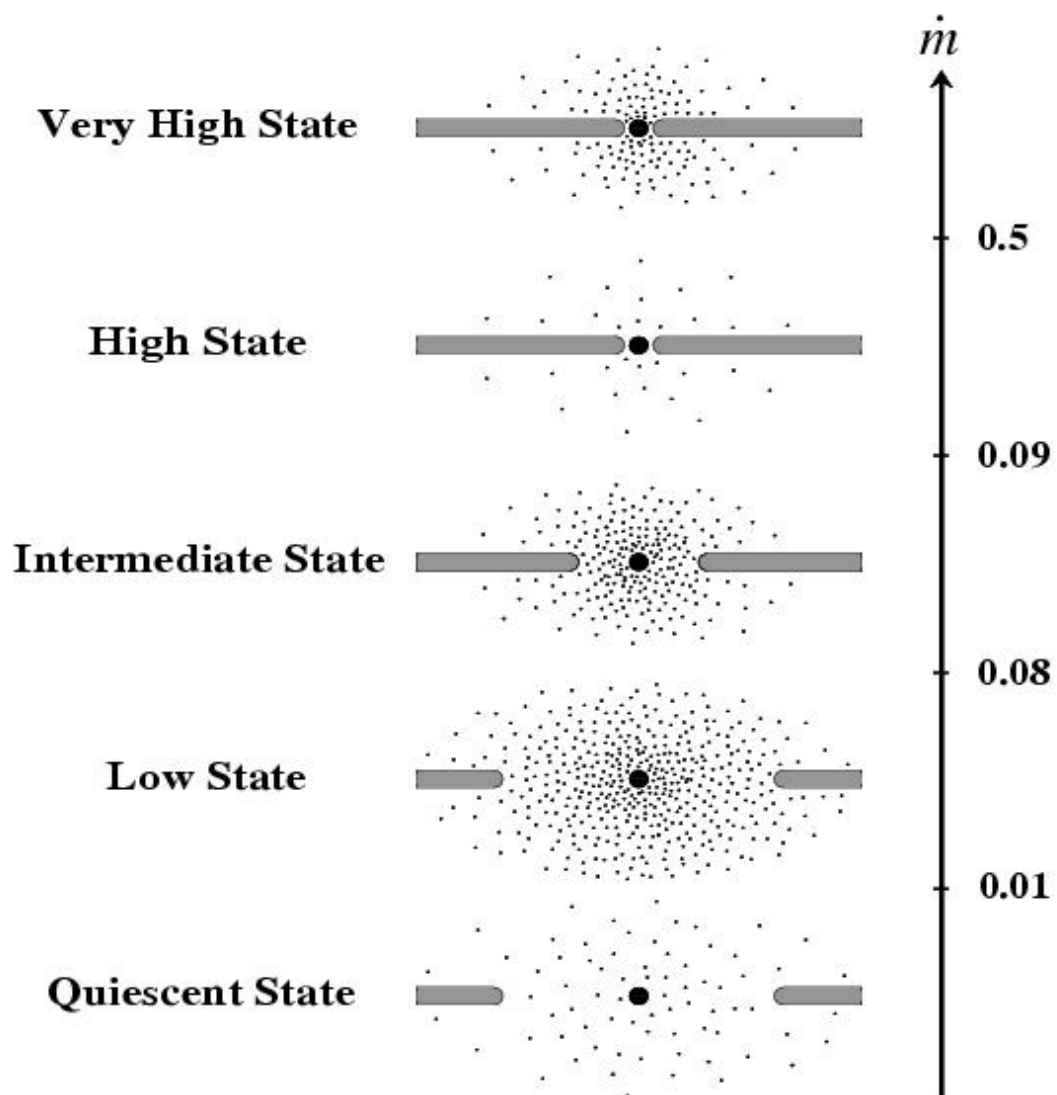
US and steeper PL at high energies

Low/Hard State (LH)

no US component; hard power-law PDS (power density spectrum); $\Gamma \sim 1.7$ (2-20keV); low luminosity; radio emission

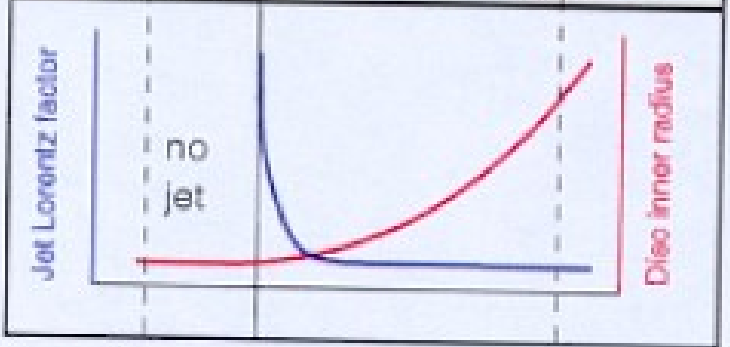
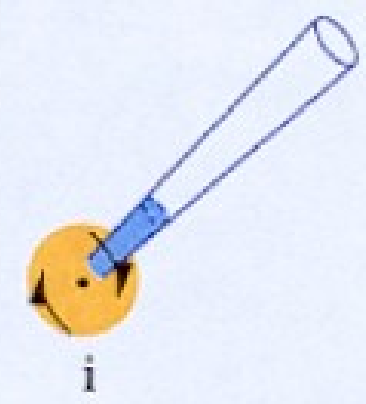
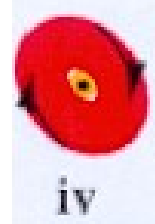
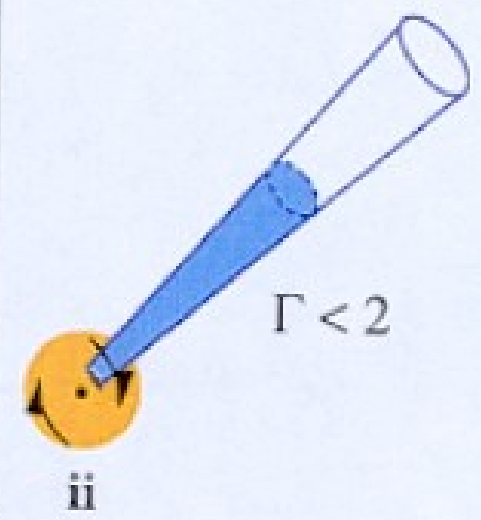
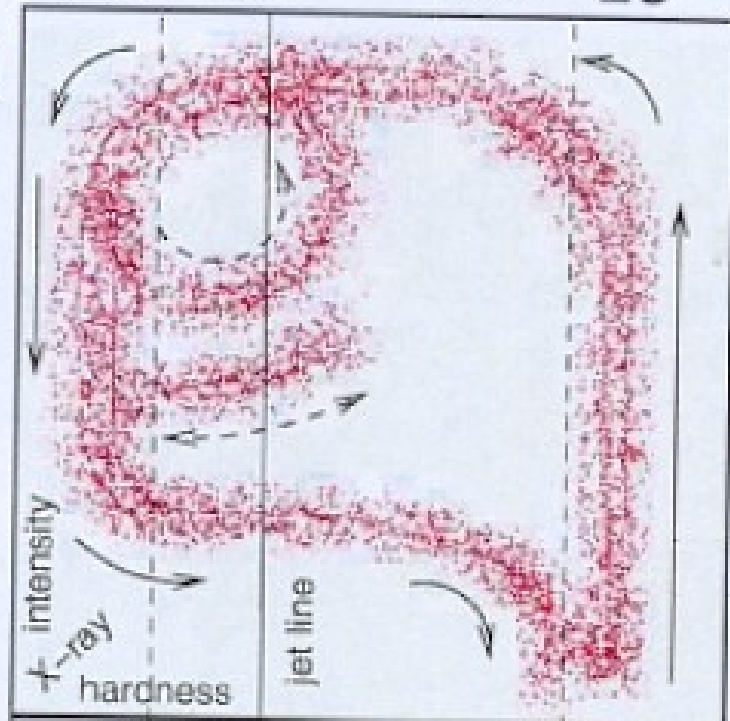
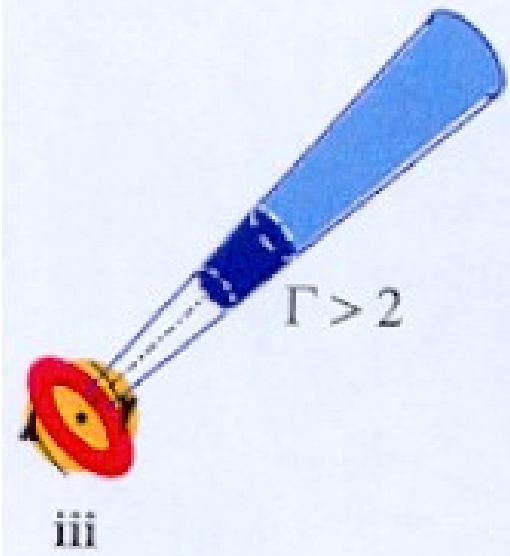
Quiescent State

truncated disk; ADAF down to the ISCO



VHS/IS

HS Soft Hard LS



iv ii i

4.1 High/Soft State and Multicolor Disk

X-ray binaries with a neutron star as compact object may have spectra that are completely different depending on whether the magnetic field of the neutron star is strong or weak.

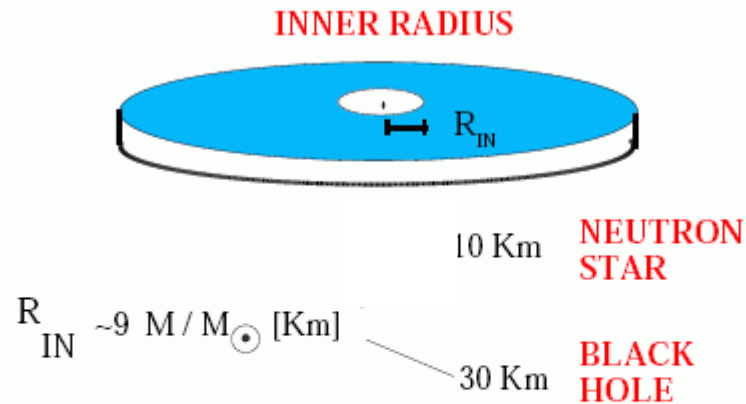
The form of the spectrum of a binary X-ray pulsar, with a surface magnetic field $> 10^{12}G$ is a flat hard power-law function with a sharp cut-off above a few tens of keV (Tanaka 1997; White et al. 1996).

The spectrum of an X-ray binary with a weakly magnetized neutron star is typically formed by the properties of the accretion disk and the neutron star envelope. The neutron star envelope contributes to the harder part of the spectrum and has a temperature of ~ 2.5 keV. Mitsuda and collaborators (1984), assuming an optically thick disk, where the energy generated by viscosity is locally dissipated in blackbody radiation, have represented the disk spectrum as a superposition of spectra with temperatures varying from a low value T_{out} at the outer edge to a maximum T_{in} at the inner edge (i.e. at the inner radius R_{in}) of the disk. This is the reason why the disk is generally called a multi-temperature or multi-color disk. By means of this model T_{in} and R_{in} can be determined through the softer part of the observed spectrum ($f(E)$), which is represented by:

$$f(E) = \frac{8\pi R_{\text{in}}^2 \cos i}{3D^2} \int_{T_{\text{out}}}^{T_{\text{in}}} \left(\frac{T}{T_{\text{in}}}\right)^{-11/3} B(E, T) \frac{dT}{T_{\text{in}}} \quad (7)$$

here i is the inclination angle of the disk, D is the distance and $B(E, T)$ is the Planck function (Shakura & Sunyaev 1973; Mitsuda et al. 1984; van Paradijs & McClintock 1996; Tanaka 1997).

X-ray binaries known to contain a black hole, proved by measurements of the mass function resulting in a mass $\geq 3 M_{\odot}$, have spectra with a soft component accompanied by a hard power-law tail (Tanaka 1997). The soft component is described by the multicolor blackbody spectrum given above and therefore it is associated with the accretion disk around the black hole. This X-ray state is defined: High/Soft. In this respect it is quite interesting to compare the different values for T_{in} and R_{in} derived in the two cases of neutron stars and black holes (Tanaka 1997). In Fig. [□](#) the values of $R_{\text{in}} \cos^{1/2} i$ obtained from the fits for accretion discs around black holes and neutron stars are collected: The projected



	Source	$R_{in} \cos^{1/2} i \text{ [Km]}$
Black holes	LMC X-1	40
	LMC X-3	24
	A0620-00	25-30
	GS2000+25	25
	GS/GRS1124-68	30
	Cyg X-1	33
	GX 339-4	17-22
Neutron stars	1608-52	6.2
	1636-53	8.0
	1820-30	6.1
	Scorpius X-1	4.1
	LMC X-2	10
	Cyg X-2	10
	Aq X-1	4

Figure 11: : **Best fit of $R_{in} \cos^{1/2} i$ for black holes and neutron stars.** From Tanaka (1997). Expected values are ~ 10 km and ~ 30 km for a neutron star and a non rotating black hole of 3 solar masses respectively.

inner radius R_{in} of accretion disks around neutron stars always results in values of ≤ 10 km, while the values for black hole binaries all are larger by a factor of 3-4 than those for neutron stars. This shows that these compact objects are indeed more massive than $3M_{\odot}$ as expected following the relationship $R_{in} \propto M_X$ (Eq. 2).

The temperature T_{in} for disks around black holes is always found to be less than ~ 1 keV, significantly lower than that for disks around neutron stars with similar luminosities. Also this difference is understood in terms of the difference in the mass M_X of the compact object: $T \propto (1/M_X)^{1/4}$ keV (Eq. 3).

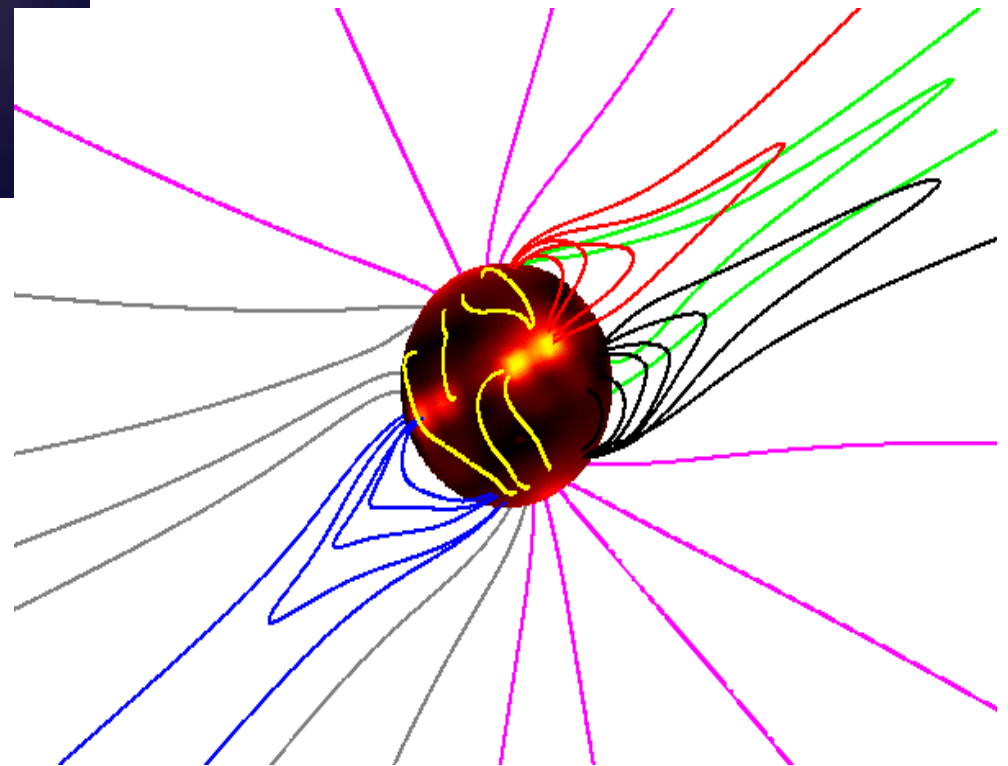
No blackbody component is present in the X-ray spectra of black hole X-ray binaries, which is consistent with the absence of a solid surface in a black hole. The second spectral component in black holes in the High/Soft state is a weak power-law with spectral index Γ , defined by the photon flux $\propto E^{-\Gamma}$ (Fig. 12). A photon index of 2.0-2.5 has been determined by Tanaka (1997) for a sample of 5 black holes. Esin and collaborators quote a range from 2.2 to 2.7. The recent review by McClintock and Remillard (2004) gives a photon index ranging from 2.1 to 4.8 for 10 black holes.

The power law component in the X-ray spectra of accreting black holes in their High/Soft state is generally interpreted as the result of inverse Compton up-scattering of low-energy disc photons by electrons with a power-law or at least a hybrid distribution (consisting of both thermal and non-thermal electrons) that can be located in coronal regions (possibly flaring) above the disc (Coppi 2000; Zdziarski et al. 2001).

Evidence for the existence of an accretion disc corona comes from systems seen almost edge on: The strong central X-ray source (i.e. the inner disc) remains hidden behind the disc rim, but X-rays are still seen. The source of emission must be quite extended because the eclipse by the companion star is only partial (White et al. 1996). The origin of accretion disc coronae is described by buoyancy of magnetic fields amplified in the disk (see Miller & Stone 2000 and references therein).



Solar Corona



5.5.2 What generates the hard X-ray luminosity?

While a thin accretion disk can account for the bolometrically dominant portion of a typical quasar SED, the hard X-rays (and the radio emission, where present) must come from something else.

Typical models invoke a “corona” above the accretion disk that produces the hard X-rays. However, models of the corona and the mechanism that produces it are only slightly above the cartoon level.

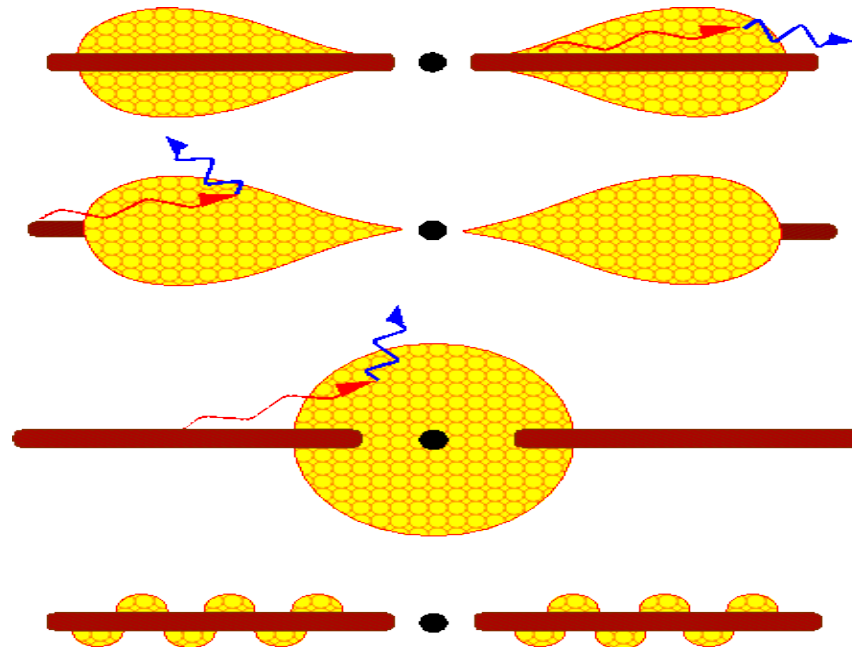


Figure 6: Suggested geometries for an accretion disk and Comptonizing corona for predominantly spectrally hard states. The top figure is referred to as a “slab” or “sandwich” geometry; however, it tends to predict spectra softer than observed. The remaining three show “photon starved geometries” wherein the corona is less effectively cooled by soft photons from the disk. The middle two geometries are often referred to as “sphere+disk geometries”, while the bottom geometry is often referred to as a “patchy corona” or “pill box” model